







Article

Biogenic Aerosol in the Arctic from Eight Years of MSA Data from Ny Ålesund (Svalbard Islands) and Thule (Greenland)

Silvia Becagli ^{1,*}, Alessandra Amore ¹, Laura Caiazzo ¹, Tatiana Di Iorio ², Alcide di Sarra ² , Luigi Lazzara ³ , Christian Marchese ^{4,5}, Daniela Meloni ², Giovanna Mori ³, Giovanni Muscari ⁶ , Caterina Nuccio ³, Giandomenico Pace ² , Mirko Severi ¹ and Rita Traversi ¹

¹ Department of Chemistry, University of Florence, Sesto Fiorentino, 50019 Florence, Italy

² ENEA, Laboratory for Observations and Analyses of Earth and Climate, 00123 Rome, Italy

³ Department of Biology, University of Florence, Sesto Fiorentino, 50019 Florence, Italy

⁴ Département de Biologie, Chimie et Géographie, Université du Québec à Rimouski, Rimouski, QC G5L 3A1, Canada

⁵ ARCTUS Inc., Rimouski, QC G5L 3QA1, Canada

⁶ Istituto Nazionale di Geofisica e Vulcanologia, INGV, Rome 00143, Italy

* Correspondence: silvia.becagli@unifi.it

Received: 19 April 2019; Accepted: 22 June 2019; Published: 26 June 2019



Abstract: In remote marine areas, biogenic productivity and atmospheric particulate are coupled through dimethylsulfide (DMS) emission by phytoplankton. Once in the atmosphere, the gaseous DMS is oxidized to produce H₂SO₄ and methanesulfonic acid (MSA); both species can affect the formation of cloud condensation nuclei. This study analyses eight years of biogenic aerosol evolution and variability at two Arctic sites: Thule (76.5° N, 68.8° W) and Ny Ålesund (78.9° N, 11.9° E). Sea ice plays a key role in determining the MSA concentration in polar regions. At the beginning of the melting season, in April, up to June, the biogenic aerosol concentration appears inversely correlated with sea ice extent and area, and positively correlated with the extent of the ice-free area in the marginal ice zone (IF-MIZ). The upper ocean stratification induced by sea ice melting might have a role in these correlations, since the springtime formation of this surface layer regulates the accumulation of phytoplankton and nutrients, allowing the DMS to escape from the sea to the atmosphere. The multiyear analysis reveals a progressive decrease in MSA concentration in May at Thule and an increase in July August at Ny Ålesund. Therefore, while the MSA seasonal evolution is mainly related with the sea ice retreat in April, May, and June, the IF-MIZ extent appears as the main factor affecting the longer-term behavior of MSA.

Keywords: biogenic aerosol; Arctic; MSA; sea ice extent; marginal ice zone; NAO

1. Introduction

Marine biota is one of the main atmospheric aerosol sources in the remote marine atmosphere. In particular, dimethylsulfide (DMS) produced by phytoplankton is oxidized in the atmosphere to methanesulfonic acid (MSA) and to sulfate by means of complex multiphase photochemical reactions [1,2].

Dimethyl sulfide (DMS) is of marine origin and its oxidative products are known to be one of the major components in the formation of new particles which, in turn, interact with the solar radiation affecting climate. Modeling studies (e.g., Hodshire et al., [3]) suggest that sulfate and sulfuric acid from DMS oxidation produce 4–6 times more submicron mass than MSA does, leading to a 10 times

stronger cooling through direct radiative forcing. Conversely, the contributions to cloud condensation nuclei precursors from MSA and from DMS-derived sulfate/sulfuric acid are comparable, leading to similar changes in the aerosol indirect effect [3].

While nonsea salt (nss) SO_4^{2-} has many sources in addition to biogenic activity (e.g., volcanic and anthropic), MSA is uniquely due to biogenic sources. For this reason, MSA concentration records in ice cores were used to investigate past climate through marine primary production which, in turn, is related to sea ice and other environmental parameters [4,5]. Indeed, the MSA atmospheric concentration is regulated by multiple processes that can be summarized into two main categories: (i) biotic factors such as primary productivity and phytoplankton species and (ii) abiotic factors that include air and sea temperatures, marine mixing layer depth, wind speed, sea–air exchange, atmospheric concentration of oxidants (O_3 , OH, and BrO), gas phase versus aqueous phase oxidation pathways, radiation, and, in polar regions, sea ice.

The Arctic plays an important role in the global climate system. The Arctic is warming at a rate almost two times larger than the global average rate (Serreze et al., [6] and references therein). At the same time, the Arctic sea ice area has decreased at a rate of 2.7% per decade [7]. These factors are expected to influence the primary production and biogenic compounds sea–air exchange in the Arctic Ocean [8].

Recent studies (e.g., Boyce et al., [9]) suggest that global marine primary production has been declining during the last century and is expected to decrease in association with global warming. Such a decline was not observed in Arctic waters [10] where, despite some regional differences (i.e., North Water Polynya), different processes are expected to lead to an increase in primary production with increasing temperatures. The decline in sea ice extent, coverage, and thickness observed in the Arctic over the past decades, with its anticipated disappearance during summer, is also expected to produce an increase in primary production [10,11].

Due to the climatic relevance of MSA, the study of the environmental parameters affecting its atmospheric concentration is particularly important. This work aims to quantify the biogenic aerosol in the Arctic and to study its seasonal evolution in relation to sea ice parameters. Particular attention is devoted to study the 8-year trend of biogenic aerosol and its response to sea ice retreat in the Arctic due to global warming.

2. Methods

2.1. Aerosols Sampling Sites

The aerosol sampling was performed at Gruebadet laboratory located at ~50 m a.s.l. at Ny Ålesund (Svalbard Islands—78.9° N, 11.9° E) and at the Thule High Arctic Atmospheric Observatory (THAAO) located in Thule (Greenland—76.5° N 68.8° W). Both sampling sites are a few kilometers away from the closest village. Figure 1 shows the map of the Arctic with the two sampling sites.

The aerosol sampling was performed at both sites by means of a TECORA Skypost sequential sampler equipped with a PM_{10} sampling head operating following the EN 12341 European rules (air flow: 2.3 m^3/h ; actual conditions). Aerosol samples were collected on Teflon (PALL Gelman) filters. The sampling started in 2010 at both sites. At Ny Ålesund, the sampling was performed with a 24h resolution only in the period of March to September, while at Thule the sampling was carried out with a 48-h resolution continuously all year round. Some interruptions occurred occasionally at the two sites due to technical problems.

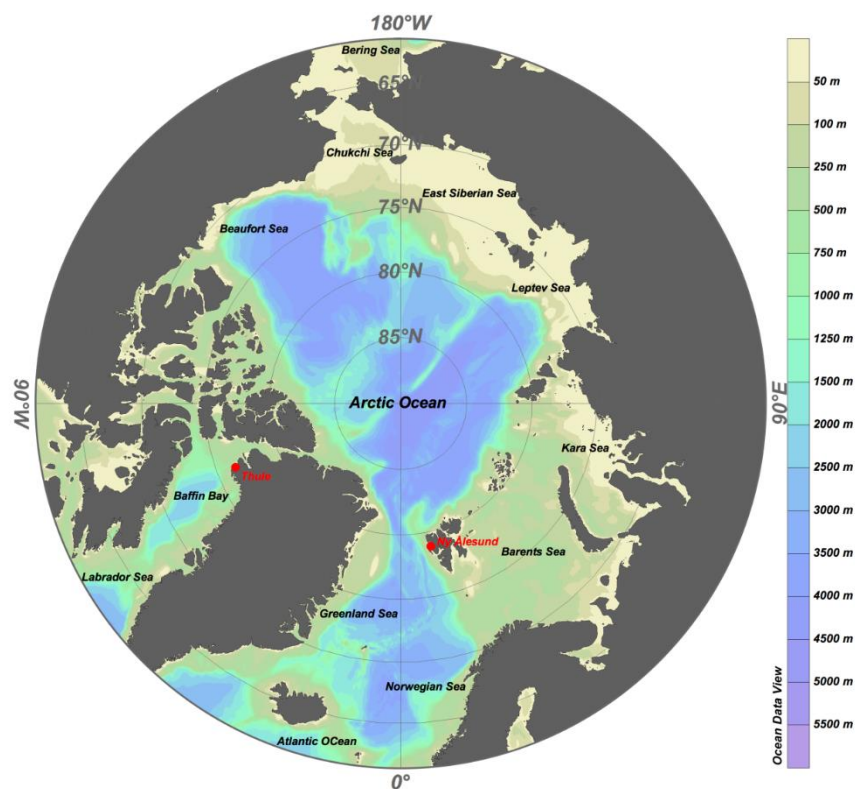


Figure 1. Map of the Arctic with the sampling sites.

2.2. Chemical Analysis

The PM_{10} mass was determined by weighing the filter before and after the sampling by means of a 5-digit microbalance (Sartorius ME235P). The filters were conditioned for 48 h (25 °C and 50% relative humidity) before weighing. Uncertainties on mass concentrations are less than 5%.

Half of each filter was extracted with 10 mL of ultrapure water (18 M Ω Milli-Q) in ultrasonic bath for 20 min. MSA was determined by ion chromatography together with the other anions and cations following the procedure described by Becagli et al. [12]. For MSA, reproducibility on real samples was better than 5%. Filter blank concentrations for methanesulfonate were always below the detection limit (0.1 μ g/L).

2.3. Sea Ice Data

Monthly average sea ice data (extent and coverage) were obtained from the Sea Ice Trends and Climatologies from SMMR and SSM/I-SSMIS, Boulder, Colorado, USA: NASA DAAC at the National Snow and Ice Data Center [13].

In this paper, we calculate the monthly ice-free surface in the marginal ice zone (IF-MIZ) as the differences between sea ice extent and sea ice coverage [14]. This parameter represents the surface free of ice in the MIZ where DMS in the water can be transferred to the atmosphere.

2.3.1. Results

Figure 2 shows the MSA concentration time evolution at the two sites, with high-resolution data in red and monthly mean data in blue. In order to highlight the seasonal pattern, Figure 3 reports the monthly median values for the two sites with the associated first and third quartiles. The MSA concentration usually starts to increase in April at both sites, reaching the largest median (11.2 ng/m³ at Thule and 22.2 ng/m³ at Ny Ålesund) and mean (14.1 ng/m³ at Thule and 33.2 ng/m³ at Ny Ålesund) values in May. It is interesting to notice that the MSA concentration starts to decrease after May in Ny Ålesund, while it remains quite constant until July at Thule, and slowly decreases afterwards.

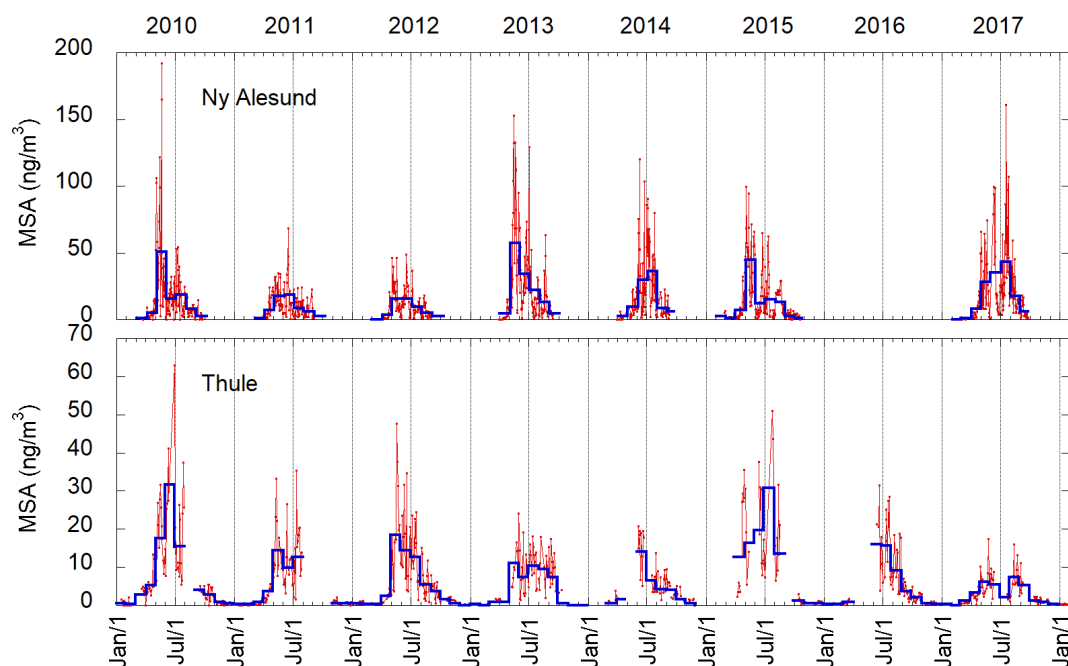


Figure 2. Methanesulfonic acid (MSA) time series at Ny Ålesund and Thule. Red lines represent high resolution data (24 h at Ny Ålesund, 48 h at Thule), blue lines are monthly mean values.

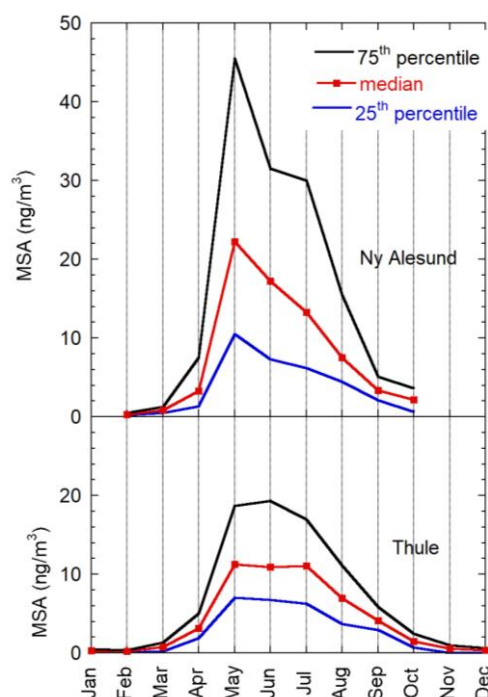


Figure 3. MSA median seasonal pattern at Ny Ålesund and Thule. Red lines represent median values, blue and black lines represent 25th and 75th percentiles, respectively.

Additional useful information that can be obtained from the high resolution data reported in Figure 2 is that in some years at Thule the MSA concentration rises already in March. These early increases recorded at Thule could be due to the presence of the North Water (NOW) Polynya in the Northern part of Baffin Bay. The presence of this very large polynya serves as a hotspot for both productivity and biodiversity [15]. In fact, the NOW polynya constitutes a key habitat for apex predators [16]. In this area, the phytoplankton bloom in March may be favored by the early solar irradiation on the sea ice free surface seawater and by the upwelling of nutrient-rich water [16,17].

In particular, the surface water exposure to solar radiation much earlier than the adjacent ice-covered waters provides favorable conditions for pelagic primary producers [18]. The polar under-ice algal communities, whose bloom precedes the pelagic one by two weeks to one month [19–21], are relevant dimethyl-sulfoxide (DMS) producers, as recently highlighted [11], and can show significantly larger DMS:chlorophyll ratios than the corresponding phytoplanktonic ones [22]. Dinoflagellates and other flagellates, as well as sea ice algae in the polynya, can therefore be responsible for the MSA concentration increase at Thule already in March and April, when the sea ice melting is very low, even though the larger DMS production occurs in May–June at the marginal ice zone (MIZ) areas. Indeed, MSA concentration maxima are usually found during May–June at both sites.

As mentioned above, the interaction of biogenic aerosol with solar radiation induces both direct and indirect effects, which may produce relevant consequences on climate. The quantification of the biogenic aerosol role in the PM₁₀ budget is therefore an important contribution towards a better understanding of the complex processes related with the Arctic climate.

By using the approach of the minimum ratio, Udisti et al. [23] obtained a nssSO₄²⁻/MSA biogenic ratio (nssSO₄²⁻/MSA)_{bio} = 3. This value agrees with the minimum values obtained in the model study by Hodshire et al. [3], who found that biogenic sulfate concentrations are 4–6 times larger than MSA.

In fact, many factors influence the (nssSO₄²⁻/MSA)_{bio} ratio; in addition, the MSA concentration is not a conservative tracer for sulfate from DMS. The influencing factors are: temperature, solar radiation, oxidant species concentration in the atmosphere (e.g., O₃, HO, NO₂, and halogen compounds), and especially the presence of clouds and water vapor in the marine boundary layer [2]. An advanced modeling study [2] shows that the DMS oxidation by aqueous-phase processes leads to a significant reduction of the SO₂ yield (and therefore sulfate) and an increase of the MSA yield, producing a lower (nssSO₄²⁻/MSA)_{bio} ratio [2]. Conversely, large background O₃ and NO₂ concentrations induce an enhancement of SO₂ production and MSA oxidation, leading to a higher (nssSO₄²⁻/MSA)_{bio} ratio [2]. For these reasons, we use a range of values for the (nssSO₄²⁻/MSA)_{bio} in the calculation of biogenic aerosol arising from the DMS oxidation (S-BioAer).

Considering a range from 3 to 6 for the (nssSO₄²⁻/MSA)_{bio} ratio, it is possible to calculate the S-BioAer concentration by means of the following equation.

$$\text{S-BioAer} = (\text{nssSO}_4^{2-}/\text{MSA})_{\text{bio}} \times \text{MSA} + \text{MSA}. \quad (1)$$

The results obtained by applying this equation to our data from Thule and Ny Ålesund are reported in Table 1. Biogenic aerosol shows a lower concentration and a smaller contribution to PM₁₀ at Thule with respect to Ny Ålesund. A larger MSA concentration (and therefore biogenic aerosol) at Ny Ålesund with respect to other Arctic sites, such as Barrow and Alert, was already found by Sharma et al. [24]. These authors [24] conclude that the large MSA concentrations measured at Ny Ålesund are due to its proximity to highly productive sea areas (MIZ in the eastern Arctic, open North Atlantic region and Barents seas) more than to atmospheric factors, such as the boundary mixing layer height (BMH). The effect of the BMH is not relevant for the two sites here considered, as both of them are coastal sites located below the BMH (50 m a.s.l. Ny Ålesund and 220 m a.s.l. Thule). Therefore in agreement with Sharma et al., [24], the larger biogenic aerosol concentration at Ny Ålesund with respect to Thule can be related to the different distance of the two sites to high productivity regions. The mean S-BioAer contribution during spring and summer is quite low but not negligible. Moreover, if the May–July mean is considered instead of the April–August mean, an increase in concentration and especially contribution to PM₁₀ is observed at both sites. This is due to the generally large MSA concentration measured during May–July and the decreasing of the contribution from other aerosol sources during this time period. The biogenic aerosol role with respect to the total aerosol amount is not negligible and has to be considered in the evaluation of the climatic effect of this type of aerosol.

Table 1. Biogenic aerosol (S-BioAer), mean content (and its standard deviation), and contribution to PM₁₀ at Thule and Ny Ålesund during the periods April–September and May–July. The values are calculated considering the values 3 and 6 for the $(\text{nssSO}_4^{2-}/\text{MSA})_{\text{bio}}$ ratio in Equation (1).

	Thule S-BioAer		Ny Ålesund S-BioAer	
	ng/m ³	% of PM10	ng/m ³	% of PM10
$(\text{nssSO}_4^{2-}/\text{MSA})_{\text{bio}} = 3$ Mean ± Std Dev. Apr–Sep	41.3 ± 36.5	1.8 ± 1.6%	72.8 ± 92.7	2.7 ± 3.5%
$(\text{nssSO}_4^{2-}/\text{MSA})_{\text{bio}} = 6$ Mean ± Std Dev. Apr–Sep	72.4 ± 63.8	3.1 ± 2.8%	127.4 ± 162.3	4.8 ± 6.1%
$(\text{nssSO}_4^{2-}/\text{MSA})_{\text{bio}} = 3$ Mean ± Std Dev May–Jul	57.2 ± 39.4	2.6 ± 1.8%	105.4 ± 109.0	4.1 ± 4.2%
$(\text{nssSO}_4^{2-}/\text{MSA})_{\text{bio}} = 6$ Mean ± Std Dev May–Jul	100.1 ± 69.0	4.5 ± 3.1%	184.5 ± 190.7	7.1 ± 7.4%

2.3.2. Sea Ice–Biogenic Aerosol Interconnection

As observed above, the MSA concentrations at the considered sites start to increase in April when sea ice starts to melt. Traditionally, in the subpolar North Atlantic Sea, the onset of the phytoplankton blooms has been attributed to changes in the mixed layer depth (MLD). The link between MLD depth, phytoplankton succession, and DMS production is a complex issue [25]. The solar radiation dose in the ocean upper mixed layer drives both phytoplankton biomass and DMS concentrations at high-latitude marine regions [26]. In open ocean/deep water the bloom begins when the mixed layer becomes shallower (from winter to spring) than the critical depth at which the phytoplankton net growth becomes positive (i.e., the growth of phytoplankton exceeds autotrophic respiration). This theory is known as the “critical depth hypothesis” [27]. Nowadays, the Sverdrup’s critical-depth hypothesis remains a widely accepted theory and it has been used to investigate the timing of the spring bloom over high-latitude regions (e.g., Henson et al., [28]). However, contemporary studies have agreed with [29], challenged [30,31], or merely refined the Sverdrup’s model by testing if reduction in turbulent mixing within the mixed layer (rather than the decrease in the mixed layer itself) can create the appropriate conditions for the bloom onset [32,33].

Ice melting adds complexity to the usual open sea picture of phytoplankton bloom and DMS releases by promoting a strong salinity-based stratification and an early phytoplankton bloom [34].

In this framework, in this section we investigate the relationship between MSA atmospheric concentration and sea ice related parameters (sea ice area: SIA; sea ice extent: SIE; and the ice-free surface in the marginal ice zone: IF-MIZ).

Figure S1 and Table 2 show that sea ice seems to play a quite different role during different months. In spring, from the beginning of the melting season until June, the biogenic aerosol concentration appears inversely correlated with SIE and SIA, suggesting that a reduced sea ice surface leads to larger productivity and to larger MSA atmospheric concentrations. This process can be explained by the fact that an isolated layer of fresher water is formed following the ice melting. This layer acts as a highly irradiated trap for organisms and nutrients, episodically entrained from below, and as a lid on the more productive underneath waters [35]. This upper marine layer plays a key role in regulating the DMS flux to the atmosphere. The correlation between MLD formation in the marginal ice zone and DMS production is also related with (i) the development of small flagellates, coccolithophores, and dinoflagellates, as most of them are strong DMSP producer in the MLD [25], and (ii) the potential limitation of DMS consumption and higher DMSP to DMS conversion efficiency due to more intense UV-B radiation in this layer [25].

Table 2. Correlation parameters and significance of correlations between monthly mean MSA (at Ny Ålesund and Thule) and the two factors sea ice area (SIA) and sea ice extent (SIE). Two time periods are considered: April, May, and June (AMJ), and July and August (JA). The correlation between MSA and the ice-free area in the marginal ice zone (IF-MIZ) is also indicated but for the April–August time period.

	MSA Thule				MSA Ny Ålesund			
	Slope	R	n.	p	Slope	R	n.	p
SIA (AMJ)	−1.94	0.548	20	<0.05	−4.18	0.720	18	<0.01
SIE (AMJ)	−2.30	0.550	20	<0.05	−4.98	0.722	18	<0.01
SIA (JA)	+0.732	0.180	13	-	+6.69	0.628	13	<0.05
SIE (JA)	+0.948	0.285	13	-	+4.87	0.557	13	<0.05
IF-MIZ	+7.39	0.444	33	<0.01	+16.3	0.426	31	<0.05

It has to be noticed that the outlier test was applied to the MSA data set in the correlation between MSA and sea ice parameters in order to exclude anomalously large values. Applying this procedure, values larger than 22 ng/m³ and 39 ng/m³ for Thule and Ny Ålesund, respectively, were excluded from the correlation (Figure 1S). A possible explanation for the missing correlation for these points is that specific fast transport processes from the Barents Sea are capable of inducing an anomalous increase in the MSA concentration [14,24].

In July and August, when the sea ice area is near to its minimum, we find a less significant positive, or completely absent, correlation between SIE or SIA and MSA in the atmosphere. Indeed, in late spring or early summer, nutrients become exhausted in the euphotic zone, the growth slows, and the loss due to increasing grazing pressure reduces phytoplankton abundance. The disappearance of the correlation in June–August could also be due to the latitudinal location of MIZ with respect to the sampling site: in summer MIZ is located north of the sampling site and southerly transport pathways are scarce [24]. A similar pattern was already found by Sharma et al. [24] at Ny Ålesund for the period of 1991 to 2004. Even though the sampling site at Ny Ålesund reported in Sharma et al. [24] (Zeppelin station, 480 m a.s.l.) is not the same as in this study (Gruvebadet 50 m a.s.l.), here we extend to the period 2010–2018 the evidence of a negative correlation between MSA and SIE in April–June and a positive (albeit less significant) correlation for July–August.

In spite of the inverse correlation between SIA (SIE) and MSA in spring over the 8-year time period, we do not observe an MSA increase as SIE decreases (Figure 4). Conversely, a decreasing trend in MSA concentration is observed in May at both sites. Such a decreasing trend is significant only at Thule, and not at Ny Ålesund due to the large variability of the MSA data and the relatively short considered time period (8 years). Therefore, the sea ice retreat in spring is able to promote the DMS production in the marine mixed layer only at seasonal scale. Indeed, the driving parameter for the DMS production and its emission into the atmosphere appears to be the IF-MIZ extent, which decreases in May leading to the reduction of DMS to the atmosphere (as demonstrated by the positive correlation between MSA and IF-MIZ).

Concerning the July–August multiyear MSA concentration at Thule, we do not observe any significant trend. Conversely, at Ny Ålesund, a significant increasing trend is observed for the time period considered here (2010–2017), confirming and extending the positive trend observed by Sharma et al. [24], for the years 1998–2004 at the Zeppelin site in Ny Ålesund. It is interesting to notice that such as increasing trend in MSA concentration in July and August at Ny Ålesund is not related to a decreasing trend in SIA (SIE) or to the increasing in IF-MIZ area in the corresponding months.

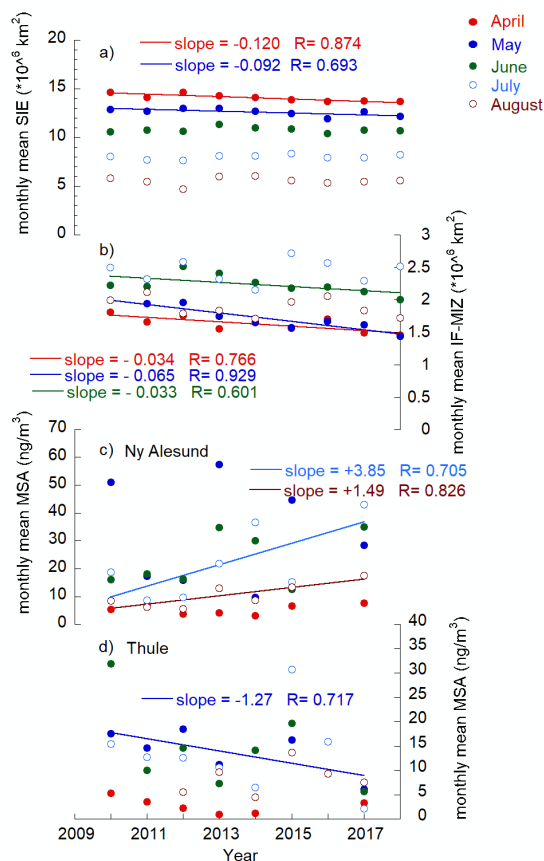


Figure 4. Monthly mean SIE (a), IF-MIZ (b), and MSA at Ny Ålesund (c) and MSA at Thule (d) as function on year. Only significant correlation ($p < 0.05$) are reported in each plot.

2.3.3. North Atlantic Oscillation–Biogenic Aerosol Interconnection

In this section, we investigate the potential interconnection between biogenic aerosol production and large-scale climate indices such as the North Atlantic Oscillation (NOA). Several studies (e.g., Henson et al., [28], Zhai et al., [36]) report links between NOA and changes in the timing of the subpolar bloom.

The mechanisms underpinning this relationship are identified to be anomalous wind-driven mixing conditions associated with NAO. In positive NAO phases, strong westerly winds produce deep mixed layers, delaying by 2 to 3 weeks with respect to NAO negative phases the start of the subpolar spring bloom. The bloom phenology (i.e., initiation, climax, and termination) is found to be strongly correlated with the mixed layer depth [28]. In fact, the dependence of MSA concentrations on wind velocity is complex. Wind strength not only controls the depth of the MLD, but also the DMS flux from seawater to the atmosphere. The two processes have an opposite effect on the MSA atmospheric concentration: strong winds produce a deep mixed layer, inducing a reduction of the DMS production in seawater; on the other hand, the DMS flux to the atmosphere increases as winds increase on the ocean surface [37,38]. Since we observe an inverse correlation between MSA and wind intensity (which is related to NAO), we assume that the wind effect on the MDL to be dominant.

Figure 5 reports the correlation between monthly values of NAO and MSA from April to August at Thule and Ny Ålesund. A significant inverse correlation between MSA concentration and NAO is found at Thule, whereas no correlation is evident at Ny Ålesund.

The fact that we find a correlation with NAO at Thule and not at Ny Ålesund could be due to a different sensitivity to westerly winds or to other factors affecting air mass transport toward Ny Ålesund, making the link between NAO and MSA more complex. In fact, the impact of NAO on MSA concentrations measured at Thule could be due to different atmospheric circulation patterns, similar to

those observed at Alert [24]. At Alert [24] found that a shift of the DMS source areas toward more productive areas is observed as NAO values become lower.

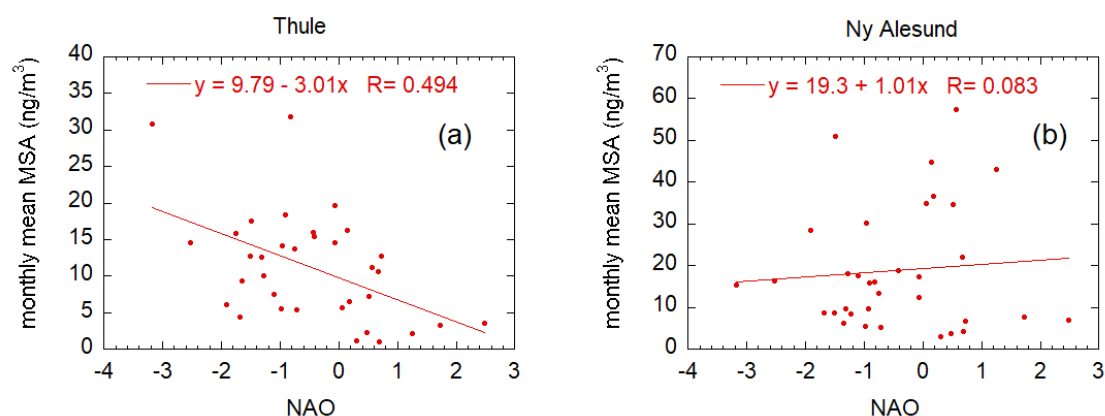


Figure 5. Correlations between monthly mean values of MSA and the North Atlantic Oscillation (NAO) index at Thule (a) and at Ny Ålesund (b).

3. Summary and Conclusions

In this work, we investigate the seasonal and 8-year long pattern of biogenic aerosol in the Arctic based on chemical analysis of PM₁₀ samples collected at two Arctic sites: Thule (76.5° N, 68.8° W), in North Western Greenland, and Ny Ålesund (78.9° N, 11.9° E), in the Svalbard Islands.

In remote areas, biogenic productivity and atmospheric particulate are related through dimethylsulfide emission by phytoplankton. Once in the atmosphere, DMS is oxidized to produce H₂SO₄ and methanesulfonic acid. The study of biogenic aerosol concentration levels and their time evolution is an important topic, due to the influence of these oxidized sulfur compounds on climate. They influence climate by direct negative radiative forcing and as a source of cloud condensation nuclei, especially over the open ocean. These climatic effects are of particular interest in the Arctic where climatic variations are amplified with respect to other regions of the Earth [24].

At both Arctic sites, MSA shows a clear seasonal pattern, with concentration maxima in summer. The MSA concentration usually starts to increase in April at both sites, with a few exceptions at Thule, where concentration can occasionally start increasing in March. The early increases recorded at Thule could be due to the presence of the North Water Polynya in the Northern part of Baffin Bay, which provides favorable conditions for primary producers by exposing surface water to solar radiation much earlier than in the adjacent ice-covered waters [15].

A $(nssSO_4^{2-}/MSA)_{bio}$ value in the range of 3 to 6 was assumed, obtained by the approach of the minimum $nssSO_4^{2-}/MSA$ ratio proposed by Udisti et al. [23] and by a model study by Hodshire et al. [3]. Using this ratio we calculated the total amount of biogenic aerosol derived from DMS oxidation (i.e., $nssSO_4 + MSA$).

In the period May–June, considering the minimum $(nssSO_4^{2-}/MSA)_{bio} = 3$ the total amount of biogenic aerosol was 57.2 ± 39.4 ng/m³ at Thule and 105 ± 109 ng/m³ at Ny Ålesund corresponding to $2.6 \pm 1.8\%$ and $4.1 \pm 4.2\%$ of PM₁₀, respectively. Although these amounts and fractions could be underestimated by the use of the minimum $(nssSO_4^{2-}/MSA)_{bio}$, the biogenic aerosol contribution is not negligible and could play an important role.

Sea ice plays a key role in determining the MSA concentration in polar regions. In spring, from the beginning of the melting season until June, the biogenic aerosol concentration appears inversely correlated with Sea Ice Extent (SIE) and Sea Ice Areas (SIA), suggesting that a lower sea ice surface leads to larger productivity and larger MSA atmospheric concentrations.

This could be due to the surface stratification induced by sea ice melt. The formation of this stable surface layer regulates the entrainment into the upper layer of cells and materials coming from the more productive waters below, and allows the DMS to escape from the sea into the atmosphere.

This is confirmed by the positive correlation between MSA and the extent of the ice-free area in the marginal ice zone over the whole summer period. In July and August, the inverse correlation between MSA and SIA (SIE) becomes less significant or even positive at both sites. As previously discussed by Sharma et al. [24], this is likely due to the different position of the MIZ with respect to the sampling sites. Due to the scarce occurrence of southerly transport processes, the correlation between MSA and SIA (SIA) disappears. These results confirm the previous study by Becagli et al. [14] carried out over a 3-year period. It may be expected that decreasing SIA and SIE trends due to global warming could lead to an increasing MSA. Experimental data reported here, however, reveal a MSA concentration decreasing trend in May (especially at Thule) when concentration maxima are measured. Therefore, the MSA production on the seasonal scale appears to be related to the retreat of sea ice in April, May and June (inverse correlation of MSA vs. SIA and vs. SIE), but the IF-MIZ extent is likely to be the main factor affecting the MSA concentration multiyear trends. Indeed, other than SIA and SIE, in May, the IF-MIZ area decreases over the 8-year period here considered, leading to a smaller production of DMS, and therefore MSA.

An increasing trend in MSA concentration is observed in July and August at Ny Ålesund for the 2010 to 2017 period, confirming and extending the trend already observed by Sharma et al. [24]. Such an increasing trend is not related to sea ice parameters that do not show in this time any significant increasing or decreasing trend.

In addition to sea ice melting, the formation of the mixed layer depth is related to the wind intensity. Indeed, the positive NAO phases lead to strong westerly winds, which in turn results in deep mixed layers, reducing the bloom intensity and therefore the DMS emission. This could be the cause for the inverse correlation between MSA and the North Atlantic Oscillation index found at Thule. Such an inverse correlation is not found at Ny Ålesund, possibly because of different sensitivities to the surrounding sea sectors, to the westerly wind, or to other factors affecting air mass transport processes toward Ny Ålesund, making the link between NAO and MSA more complex.

These differences between sites suggest that the ongoing environmental changes are not geographically homogeneous and can produce different effects. Therefore, to better understand how environmental changes will affect phytoplankton dynamics and DMS fluxes, it is becoming increasingly necessary to have targeted observational programs that must be conducted on specific regional studies.

The interconnection between sea ice extent, NAO and biogenic aerosol production has a strong climatic importance and deserves further studies, in particular based both on long-term measurements and modeling studies. These studies should include also other atmospheric and oceanic data in order to understand the ocean–atmosphere interconnections and predict the effect of climate change on such a sensitive environment.

Supplementary Materials: The following are available online at <http://www.mdpi.com/2073-4433/10/7/349/s1>, Figure S1.

Author Contributions: Conceptualization, S.B.; Data curation, G.P., M.S. and R.T.; Investigation, TDI, A.D.S., L.L., C.M., D.M., G.M., C.N., M.S., and R.T.; Methodology, A.A., L.C., A.D.S., C.M., C.M., G.M., G.P.; Writing—original draft, S.B.

Funding: This research was partially funded by the Italian Ministry of University and Research (MIUR) within the framework of the projects *Dirigibile Italia: una piattaforma per lo studio multi-disciplinare dei cambiamenti climatici nella regione artica e della loro influenza sulle medie latitudini* (PRIN-2007); *ARCTICA-ARCTic Research on the Interconnections between Climate and Atmosphere* (PRIN 2009); *Observations of changes in chemical composition and physical properties of Polar Atmospheres from NDACC Stations* (PNRA 2010–2012); *ARCA-Arctic: present climatic change and past extreme events* (MIUR 2014–2016); *SVAAP—The study of the water vapor in the polar atmosphere* (PNRA 2015–2016); *OASIS-YOPP—Observations of the Arctic Stratosphere In Support of YOPP* (PNRA 2016–2018).

Acknowledgments: The logistic assistance of the Polar Support Unit of the CNR Department of Earth and Environment (POLARNET) to the activity at Ny Ålesund is gratefully acknowledged.

Conflicts of Interest: The authors declare no conflict of interest.

References

1. Gondwe, M.; Krol, M.; Klaassen, W.; Gieskes, W.; de Baar, H. Comparison of modeled versus measured MSA:nssSO₄ ratios: a global analysis. *Glob. Biogeochem. Cycles* **2004**, *18*, GB2006. [[CrossRef](#)]
2. Hoffmann, E.H.; Tilgner, A.; Schrödner, R.; Bräuer, P.; Wolke, R.; Herrmann, H. An advanced modeling study on the impacts and atmospheric implications of multiphase dimethyl sulfide chemistry. *PNAS* **2016**, *112*, 11776–11781. [[CrossRef](#)] [[PubMed](#)]
3. Hodshire, A.L.; Campuzano-Jost, P.; Kodros, J.K.; Croft, B.; Nault, B.A.; Schroder, J.C.; Jimenez, J.L.; Pierce, J.R. The potential role of methanesulfonic acid (MSA) in aerosol formation and growth and the associated radiative forcings. *Atmos. Chem. Phys.* **2019**, 3137–3160. [[CrossRef](#)]
4. Isaksson, E.; Kekonen, T.; Moore, J.; Mulvaney, R. The methanesulfonic acid (MSA) record in a Svalbard ice core. *Ann. Glaciol.* **2005**, *42*, 345–351. [[CrossRef](#)]
5. Becagli, S.; Castellano, E.; Cerri, O.; Curran, M.; Frezzotti, M.; Marino, F.; Morganti, A.; Proposito, M.; Severi, M.; Traversi, R.; et al. Methanesulphonic acid (MSA) stratigraphy from a Talos Dome ice core as a tool in depicting sea ice changes and southern atmospheric circulation over the previous 140 years. *Atmos. Environ.* **2009**, *43*, 1051–1058. [[CrossRef](#)]
6. Serreze, M.C.; Barry, R.G. Processes and impacts of Arctic amplification: A research synthesis. *Glob. Planet. Change* **2011**, *77*, 85–96. [[CrossRef](#)]
7. Forster, P.; Ramaswamy, V.; Artaxo, P.; Berntsen, T.; Betts, R.; Fahey, D.W.; Haywood, J.; Lean, J.; Lowe, D.C.; Myhre, G. Changes in Atmospheric Constituents and in Radiative Forcing. In *Climate Change 2007: The Physical Science Basis*; Cambridge University Press: Cambridge, UK, 2007.
8. Gabric, A.J.; Qu, B.; Matrai, P.; Hirst, A.C. The simulated response of dimethylsulfide production in the Arctic Ocean to global warming. *Tellus B* **2005**, *57*, 391–403. [[CrossRef](#)]
9. Boyce, D.G.; Lewis, M.R.; Worm, B. Global phytoplankton decline over the past century. *Nature* **2010**, *466*, 591–596. [[PubMed](#)]
10. Bélanger, S.; Babin, M.; Tremblay, J.-E. Increasing cloudiness in Arctic damps the increase in phytoplankton primary production due to sea ice receding. *Biogeosciences* **2013**, *10*, 4087–4101. [[CrossRef](#)]
11. Arrigo, K.R.; Perovich, D.K.; Pickart, R.S.; Brown, Z.W.; van Dijken, G.L.; Lowry, K.E.; Mills, M.M.; Palmer, M.A.; Balch, W.M.; Bahr, F.; et al. Massive phytoplankton blooms under Arctic sea ice. *Science* **2012**, *336*, 1408. [[CrossRef](#)] [[PubMed](#)]
12. Becagli, S.; Ghedini, C.; Peeters, S.; Rottiers, A.; Traversi, R.; Udisti, R.; Chiari, M.; Jalba, A.; Despiiau, S.; Dayan, U.; et al. MBAS (methylene blue active substances) and LAS (linear Alkylbenzene sulphonates) in Mediterranean coastal aerosols: sources and transport processes. *Atmos. Environ.* **2011**, *45*, 6788–6801. [[CrossRef](#)]
13. Stroeve, J. Sea Ice Trends and Climatologies from SMMR and SSM/I-SSMIS. Sea Ice Extent. NASA DAAC at the National Snow and Ice Data Center: Boulder, CO, USA. Available online: <http://nsidc.org/data/nsidc-0192.html> (accessed on 19 April 2019).
14. Becagli, S.; Lazzara, L.; Marchese, C.; Dayan, U.; Ascanius, S.E.; Cacciani, M.; Caiazzo, L.; Di Biagio, C.; Di Iorio, T.; di Sarra, A.; et al. Relationships linking primary production, sea ice melting, and biogenic aerosol in the Arctic. *Atmos. Environ.* **2016**, *136*, 1–15. [[CrossRef](#)]
15. Marchese, C.; Albouy, C.; Tremblay, J.-É.; Dumont, D.; D’Ortenzio, F.; Vissault, S.; Bélanger, S. Changes in phytoplankton bloom phenology over the north water (now) polynya: A response to changing environmental conditions. *Polar Biol.* **2017**, *40*, 1721–1737. [[CrossRef](#)]
16. Stirling, I. The importance of polynya, ice edges, and leads to marine mammals and birds. *J. Mar. Sys.* **1997**, *10*, 9–21. [[CrossRef](#)]
17. Smith, S.D.; Muench, R.D.; Pease, C.H. Polynyaa and leads: An overview of physical processes and environment. *J. Geophys. Res.* **1990**, *95*, 9461–9479. [[CrossRef](#)]
18. Tremblay, J.E.; Gratton, Y.; Fauchota, J.; Price, N.M. Climatic and oceanic forcing of new, net, and diatom production in the North Water. *Deep Sea Res. Part II* **2002**, *49*, 4927–4946. [[CrossRef](#)]
19. Guglielmo, L.; Carrada, G.C.; Catalano, G.; Dell’Anno, A.; Fabiano, M.; Lazzara, L.; Mangoni, O.; Pusceddu, A.; Saggiomo, V. Structural and functional properties of sea ice communities in the first year sea ice at Terra Nova Bay (Ross Sea, Antarctica). *Polar Biol.* **2000**, *23*, 137–146. [[CrossRef](#)]

20. Lazzara, L.; Nardello, I.; Ermanni, C.; Mangoni, O.; Saggiomo, V. Light environment and seasonal dynamics of microalgae in the annual sea ice at Terra Nova Bay (Ross Sea, Antarctica). *Antarct. Sci.* **2007**, *19*, 83–92. [[CrossRef](#)]
21. Levasseur, M. Impact of Arctic meltdown on the microbial cycling of sulphur. *Nat. Geogr.* **2013**, *6*, 691–700. [[CrossRef](#)]
22. Lee, P.A.; de Mora, S.J.; Gosselin, M.; Levasseur, M.; Bouillon, R.-C.; Nozais, C.; Michel, C. Particulate dimethylsulfoxide in Arctic sea-ice algal communities: The cryoprotectant hypothesis revisited. *J. Phycol.* **2001**, *37*, 488–499. [[CrossRef](#)]
23. Udisti, R.; Bazzano, A.; Becagli, S.; Bolzacchini, E.; Caiazzo, L.; Cappelletti, D.; Ferrero, L.; Frosini, D.; Giardi, F.; Grotti, M.; et al. Sulfate source apportionment in the Ny-Ålesund (Svalbard Islands) Arctic aerosol. *Rend. Fis. Acc. Lincei.* **2016**, *27* (Suppl. S1), 85–94. [[CrossRef](#)]
24. Sharma, S.; Chan, E.; Ishizawa, M.; Toom-Sauntry, D.; Gong, S.L.; Li, S.M.D.; Tarasick, W.; Leaitch, W.R.; Norman, A.; Quinn, P.K.; et al. Influence of transport and ocean ice extent on biogenic aerosol sulfur in the Arctic atmosphere. *J. Geophys. Res.* **2012**, *117*, D12209. [[CrossRef](#)]
25. Simó, R.; Pedrós-Alió, C. Role of vertical mixing in controlling the oceanic production of dimethyl sulphide. *Nature* **1999**, *402*, 396–399. [[CrossRef](#)]
26. Vallina, S.M.; Simó, R.; Gassó, S. What controls CCN seasonality in the Southern Ocean? A statistical analysis based on satellite-derived chlorophyll and CCN and model-estimated OH radical and rainfall. *Global Biogeochem. Cycles* **2006**, *20*, GB1014. [[CrossRef](#)]
27. Sverdrup, H.U. On conditions for the vernal blooming of phytoplankton. *J. Cons. int. Explor.* **1953**, *18*, 287–295. [[CrossRef](#)]
28. Henson, S.A.; Dunne, J.P.; Sarmiento, J.L. Decadal variability in North Atlantic phytoplankton blooms. *J. Geophys. Res.* **2009**, *114*. [[CrossRef](#)]
29. Mahadevan, A.; D’Asaro, E.; Lee, C.; Perry, M.J. Eddy-driven stratification initiates North Atlantic spring phytoplankton blooms. *Science* **2012**, *337*, 54–58. [[CrossRef](#)] [[PubMed](#)]
30. Behrenfeld, M. Abandoning Sverdrup’s Critical Depth Hypothesis on phytoplankton blooms. *Ecology* **2010**, *91*, 977–989. [[CrossRef](#)] [[PubMed](#)]
31. Boss, E.; Behrenfeld, M. In situ evaluation of the initiation of the North Atlantic phytoplankton bloom. *Geophys. Res. Lett.* **2010**, *37*, L18603. [[CrossRef](#)]
32. Chiswell, S.M. Annual cycles and spring blooms in phytoplankton: Don’t abandon Sverdrup completely. *Mar. Ecol. Prog. Ser.* **2011**, *443*, 39–50. [[CrossRef](#)]
33. Taylor, J.R.; Ferrari, R. Shutdown of turbulent convection as a new criterion for the onset of spring phytoplankton blooms. *Limnol. Oceanogr.* **2011**, *56*, 2293–2307. [[CrossRef](#)]
34. Marchese, C.; Castro de la Guardia, L.; Myers, P.G.; Bélanger, S. Regional differences and inter-annual variability in the timing of surface phytoplankton blooms in the Labrador Sea. *Ecol. Indic.* **2019**, *96*, 81–90. [[CrossRef](#)]
35. Galí, M.; Simó, R. Occurrence and cycling of dimethylated sulfur compounds in the Arctic during summer receding of the ice edge. *Mar. Chem.* **2010**, *122*, 105–117. [[CrossRef](#)]
36. Zhai, L.; Platt, T.; Tang, C.; Sathyendranath, S.; Walne, A. The response of phytoplankton to climate variability associated with the North Atlantic Oscillation. *Deep Sea Res. Part II* **2013**, *93*, 159–168. [[CrossRef](#)]
37. Huebert, B.J.; Blomquist, B.W.; Yang, M.X.; Archer, S.D.; Nightingale, P.D.; Yelland, M.J.; Stephens, J.; Pascal, R.W.; Moat, B.I. Linearity of DMS transfer coefficient with both friction velocity and wind speed in the moderate wind speed range. *Geophys. Res. Lett.* **2010**, *37*, L01605. [[CrossRef](#)]
38. Park, K.-T.; Lee, K.; Yoon, Y.-J.; Lee, H.-W.; Kim, H.-C.; Lee, B.-Y.; Hermansen, O.; Kim, T.-W.; Holmén, K. Linking atmospheric dimethyl sulfide and the Arctic Ocean spring bloom. *Geophys. Res. Lett.* **2013**, *40*, 155–160. [[CrossRef](#)]

